16th World Conference on Earthquake Engineering, 16WCEE 2017

Santiago Chile, January 9th to 13th 2017

Paper N° 2220

Registration Code: S-V1463182651

PUNCHING SHEAR IN WAFFLE SLABS, ANALYSIS OF EXPERIMENTAL BEHAVIOR

E. Arellano-Mendez(1), O. M. González Cuevas(2)

(1) *Professor, Department of Materials, Universidad Autonoma Metropolitana, México, eam@azc.uam.mx*
(2) *Professor, Department of Materials, Universidad Autonoma Metropolitana, México, omgc@azc.uam.mx*

…

Abstract

Eleven full-sized posttensioned waffle slab-column connections subjected to axial load and flexural moment were tested to study their mode of failure, strength and ductility. The test variables are: 1) provision of stirrups or stud shear reinforcement; 2) spacing between stirrups or shear studs; 3) slab thickness; 4) size of the solid region around the column; and 5) relationship between the applied axial load, Vu, and the punching shear strength of the slab with axial load and without shear reinforcement, VcR. Most tests carried out in this type of connections, according to a bibliographical review, used solid flat slab. In this research, waffle slabs were used, being more used in Mexico than solid slabs because economic reasons. The ductility of the connections was of special interest, since this type of structures are usually considered of low or medium ductility because the punching shear failures are brittle. It has been found that the maximum IDR (interstory drift ratio) reached in structures with flat slabs-columns connections depends on the relation between Vu and VcR, so this was one of the main variables in the research.

Keywords: shear; punching; slabs; waffle; experimental

1. Introduction

Posttensioned flat slabs may be designed or built as solid or as waffle types. In Mexico, it is most common to use waffle posttensioned slabs. Although they require more manpower, they are cheaper, since their total cost is constituted by a 40 % of manpower and 60 % of materials, while in countries like United States of America, total cost is divided between 60% manpower and 40 % materials. A waffle slab becomes generally more expensive than a solid one in these countries.

The structural design based on posttensioned waffle slabs in seismic zones was regulated in Mexico for the first time in "Normas técnicas complementarias para el diseño y construcción de estructuras de concreto" [1]. This document establishes that these structures must have a dual system; the first one is a stiff reinforced concrete structure able to resist independently the seismic actions; this system generally is built within the perimeter of the building. The second is the system of waffle slab and columns, which must be able to resist gravitational loads and the actions and interstory drift that are induced when it works altogether with the first system under the action of the earthquake, Section 9.7.3, [2].

The building practice in Mexico of posttensioned waffle slabs consists of having main ribs relatively wide in the column axis, which, when intersected with the perpendicular axis, form a solid zone around the columns. However, this solid zone is relatively small in comparison with the one that usually exists in reinforced concrete waffle slabs. It has been considered important to carry on a research program oriented to study the behavior of the connections of the columns with the posttensioned waffle slabs, with the purpose of obtaining regulations for calculating the resistance to punching shear and to determine its ductility. It is of paramount importance to estimate the interstory drift ratio that the structures with this building system can reach, without the occurrence of a connection failure.

2. Methodology

A three story structure was designed, following the current building regulations in Mexico, which is considered a ductility of 2, and with an interstory drift ratio limit of 0.06 for this system. The structure consists of six bays in two ways, with bays of 6 m each way. The structure has an exterior earthquake resistance system formed by columns of 0.8x0.8m and beams of 0.5x1.2m. The waffle slab system is formed by columns of 0.3x0.3m and a slab of 0.185m; the width of the ribs is 0.3, 0.2 and 0.1m for the main rib, adjacent and secondary respectively (view figure 1).

The test specimen is the 1.9x1.9m portion of slab taken around the node that includes the column, the main ribs and the adjacent ribs (see shaded central zone of figure 1). The details of the specimen can be seen in figures 2 and table 1. The length of the column under the slab is 1.3 m and that of the top is 1.4 m. Due to the characteristics of the test machine the specimen was rotated 90 degrees.

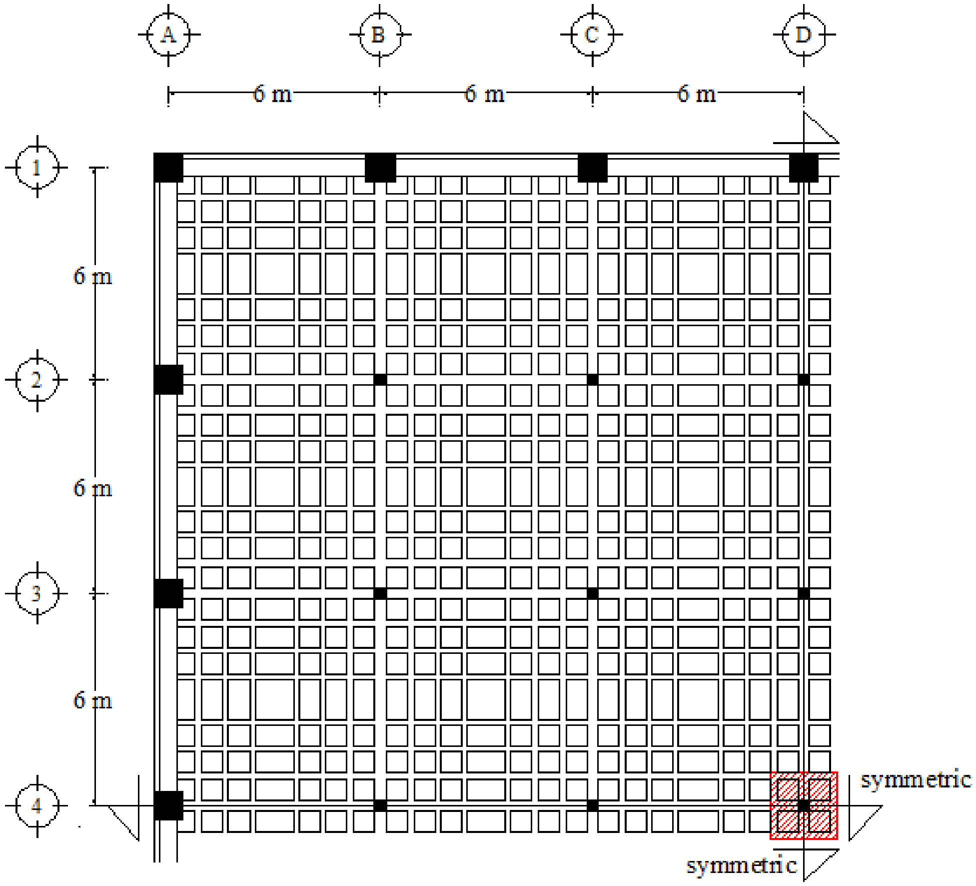

Fig. 1 – Dual system, Seismic Structure and Gravitational Structure (waffle slab)

Fig. 2 – Specimen

Table 1 – Table of reinforcement

Specimen	Principal Rib X	Principal Rib Y	Adjacent Rib	Column	Reinf. Ribs	Reinf. Cols
LP-02	2#6+2#3 +2T 0.5	2#6+2#3 +2T 0.5	2#3 +1 T 0.5	6#6	Stirrups @9	Stirrups @7
LP-03	2#6+2#3 +2T 0.5	2#6+2#3 +2T 0.5	2#3 +1 T 0.5	6#6	SSR @11	Stirrups @7
LP-04	2#6+2#3 +2T 0.5	2#6+2#3 +2T 0.5	2#3 +1 T 0.5	6#6	SSR @9	Stirrups @7
LP-05	2#6+4#3 +2T 0.5	2#6+4#3 +4T 0.5	2#3 +1 T 0.5	6#6	SSR @9	Stirrups @7
LP-06	2#6+4#3 +2T 0.5	2#6+4#3 +4T 0.5	2#3 +1 T 0.5	6#6	SSR @7	Stirrups @7
LP-07	2#6+2#3 +2T 0.5	2#6+2#3 +2T 0.5	2#3 +1 T 0.5	6#6	Stirrups @9	Stirrups @7
LP-08	2#6+2#3 +2T 0.5	2#6+2#3 +2T 0.5	2#3 +1 T 0.5	6#6	Stirrups @9	Stirrups @7

3. Displacement history

The first load applied is an axial force applied on the inferior column, which represents the punching shear [3]. In the first part of test, the load is applied in increasing form in at least 10 steps until reaching the desired value. The second part of the test is controlled by displacements (see figure 3). A interstory drift ratio objective is defined associated with the displacement of the control node. For each displacement increase, four cycles of load and unload are applied as shown in figure 3. To control the test, the control node is monitored with a displacement transducer.

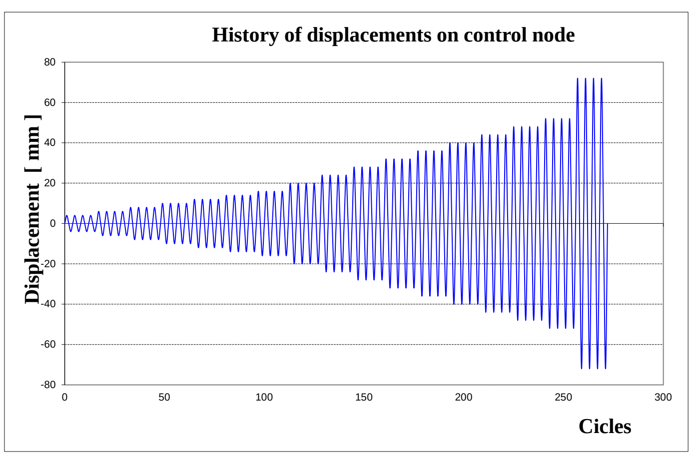

Fig. 3 – Displacement history

4. Hysteresis loop

Hysteresis loop is a representation of the force applied to achieve the displacement in the control node. The horizontal axis represent the lateral displacement Δ_{TOTAL} divided by the height (interstory drift ratio); in the vertical axis the lateral force V required to achieve the displacement is plotted, see figure 4. In the hysteresis diagrams a thinning around the zero lateral load, or pinching, can be clearly seen. This phenomenon implies that little energy is dissipated in the cycles; see figures 5a, 5b, 5c, 5d, 5e, 5f and 5g.

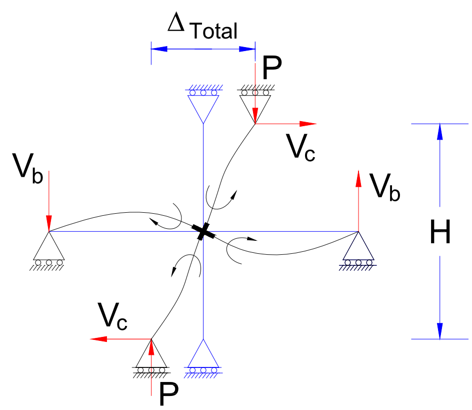

Fig. 4 – Displacement definitions

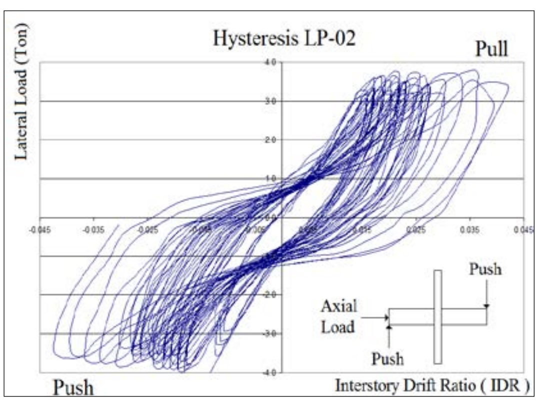

a)

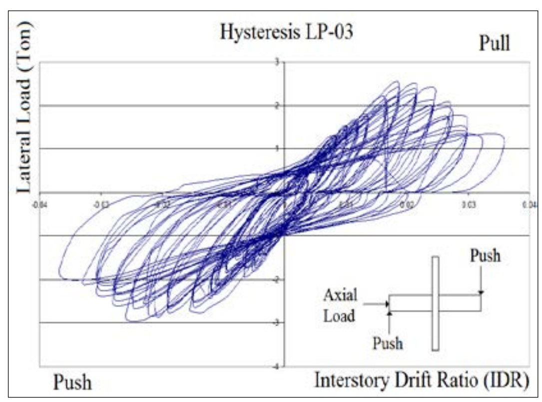

b)

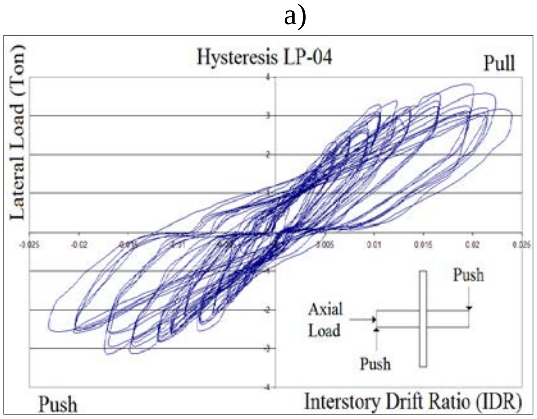

c)

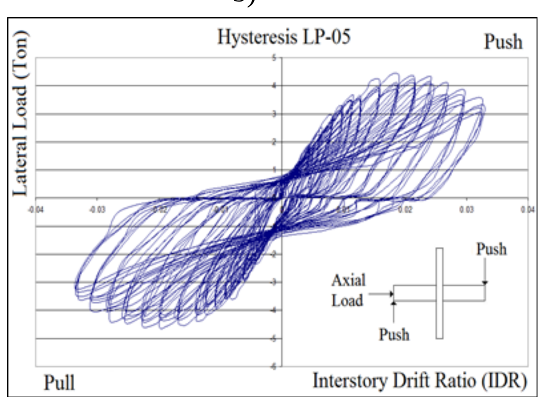

d)

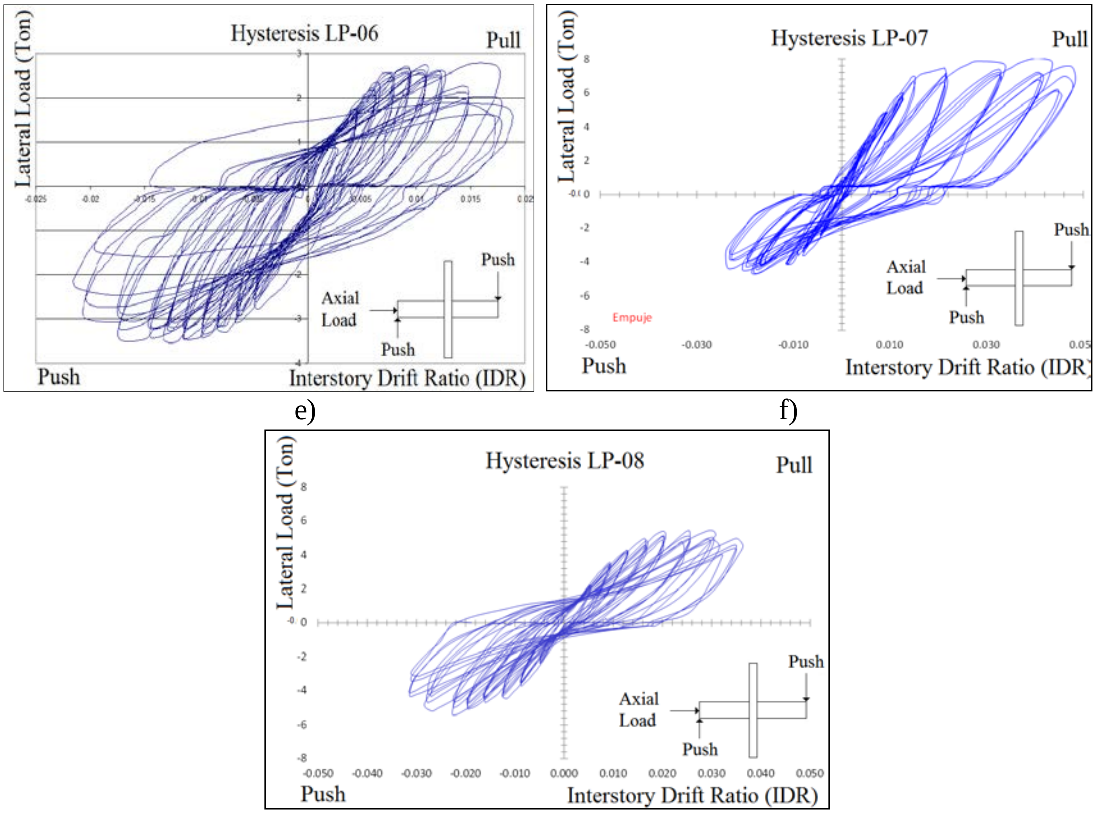

e) f)

g)

Fig. 5 – Hysteresis loop a)LP-02, b)LP-03, c)LP-04, d)LP-05, e)LP-06, f) LP-07, g) LP-08

Figure 6 shows the envelope of the hysteresis curves. The displacements corresponding to the interstory drift ratios used in the design of the structure, 0.006 and 0.012, section 1.8, [4] are shown in this figure. It can be observed that in all cases the maximum resistance is well beyond the limits used in the design, so, the design regulations appear to be conservative.

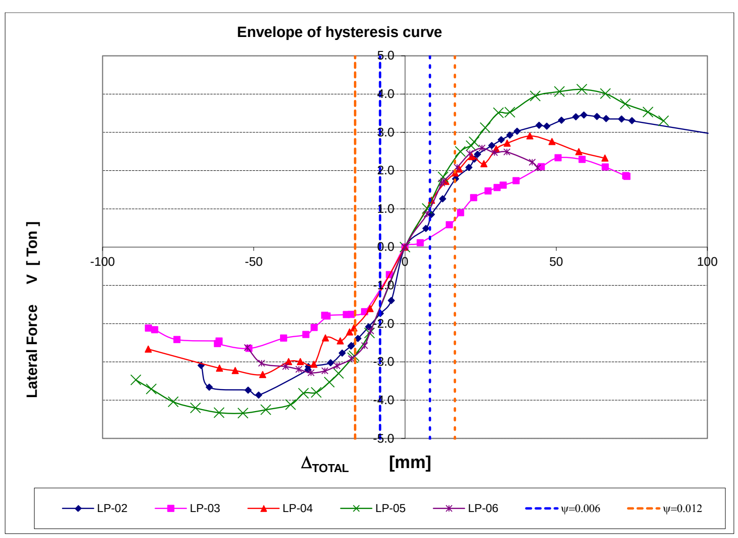

Fig. 6 – Envelope hysteresis loop

Peak-to-peak stiffness is defined as the slope in the diagram average lateral force vs total displacement, as shown in figure 7. Stiffness K is the slope of the straight line joining the maximum displacement points in the cycle; this is the stiffness of the cycle. To measure the stiffness degradation during the tests of the specimens, a normalized graphic is used where the stiffness of the cycle is divided by the initial stiffness (stiffness of the first cycle). Specimen LP-06, which was submitted to a larger axial load, presents the largest stiffness degradation, see figure 7.

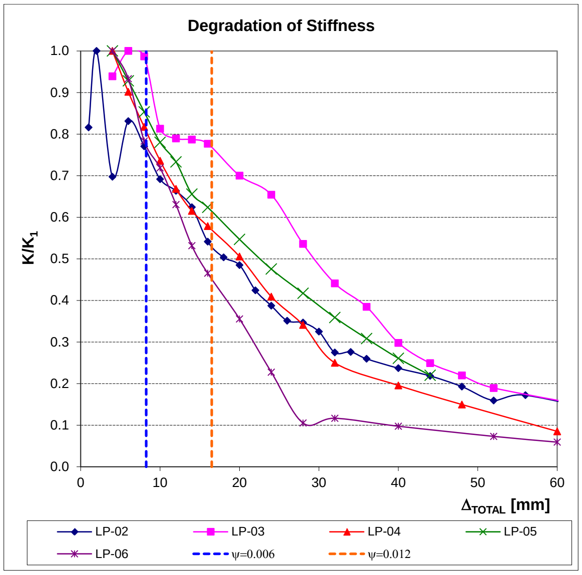

Fig. 7 – Degradation of stiffness

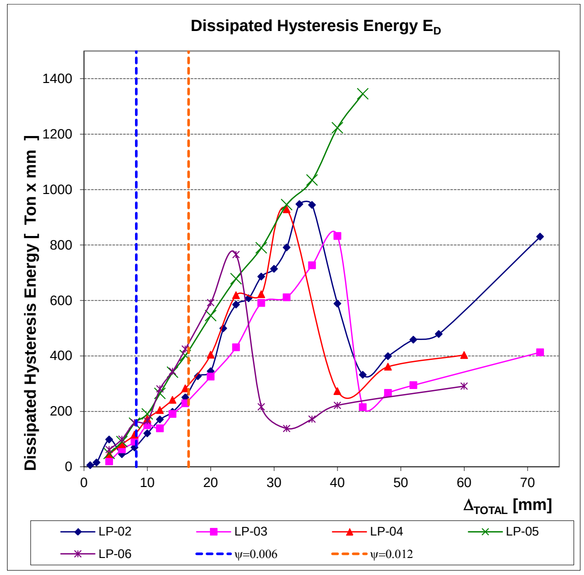

Fig. 8 – Energy Dissipated

Dissipated hysteresis energy is calculated for each cycle and defined as the area under the curve average punching shear vs. total displacement as shown in figure 8. In all specimens, the maximum value in the dissipated hysteretic energy curve corresponds to cycles beyond the limits of interstory drift ratio established in the norms [4]. It is observed that in most of the tested specimens, a sudden drop occurs after the maximum value is reached. So that maximum value corresponds to the failure of the specimen. Specimen LP-05 was the only one without the sudden drop. It should be noted that the failure mechanism in this specimen may be attributed to a flexural failure in the rib rather than a punching shear, as suggested by the cracking pattern in the specimen.

Equivalent viscous damping, (see figure 9), may be calculated in experimental curves with equation 1 [5]. This parameter represents the internal frictions in the material, which this type of connections is increased by the action of the posttensioned tendons that tends to close the cracks once the loads are removed.

$$\zeta_{eq} = \frac{1}{4\pi}\frac{E_D}{E_{So}} = \frac{1}{4\pi}\frac{\text{Energy dissipated}}{\text{Strain energy}} \tag{1}$$

Equivalent viscous damping also is a parameter of the damage accumulation in the element as the cracking increases, so does the damping. In NTC-Sismo an equivalent viscous damping of 0.05 is assumed to determine the design spectrum [4]. However, in the range of the design interstory drift ratio, the dampings measured experimentally were between 0.1 and 0.2 (see figure 9) It could be considered that the NTC lead to conservative results, something appropriate to guarantee the suitable levels of structural security.

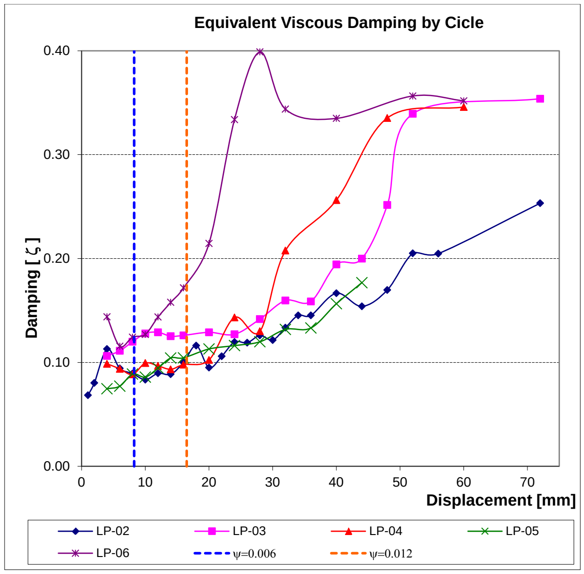

Fig. 9 – Experimental Equivalent Viscous damping

The maximum values in damping seem too high, but they are consistent with the result of tests of beam column connections [8].

To overcome the uncertainty in defining the yield displacement, the following definition is used. A graphic is obtained that represents the envelope of the hysteresis loops, meaning lateral force vs relative displacement [6, 7]. This envelope is idealized as one with elastoplastic behavior. The initial slope of the idealized behavior is secant, and is determined by joining the origin with the point where a lateral load is equal to two-third parts of the maximum shear force registered during the test (V_{test}). The idealized plastic portion of the graphic is a horizontal line passing by the maximum load point and going on to the failure displacement. This displacement is defined as the point corresponding to a decrease of 20 % in the maximum measured load. The setting of the idealized graphic could be seen in figure 9.

Ductility in the connection can be determined as the failure displacement divided by the yield displacement. (Equation 2).

$$\mu = \frac{\Delta_{u80}}{\Delta_y} \tag{2}$$

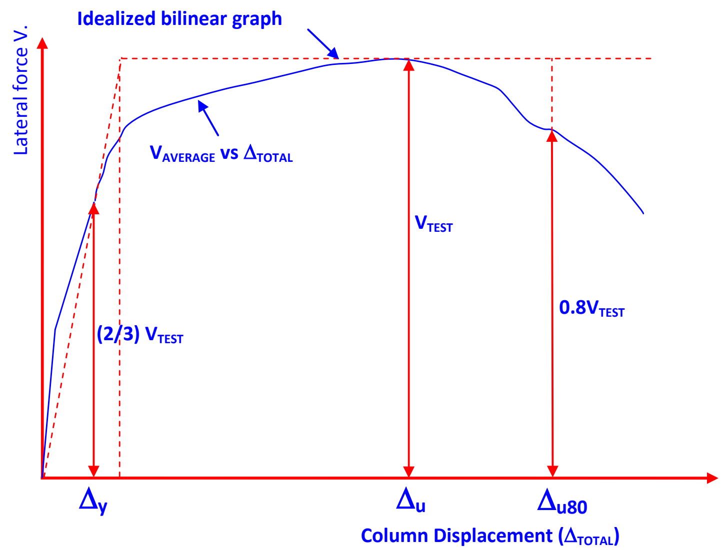

Fig. 10 – Idealized elastic-plastic behavior

The ductility of the connection was calculated using the quadrants 1 and 3, according to the procedure proposed [7]. The results of table 2 are the average of the former calculations. The values calculated are between 3.4 and 4.5. The slab-column connections of reinforced concrete have been traditionally associated with a fragile behavior, or of low ductility, but in this case of posttensioned slabs the opposite occurs.

Table 2 – Idealized elastic-plastic behavior

Esp.	Δ_y (mm)	Δ_u (mm)	Δ_{u80} (mm)	μ	V_y (ton)	V_u (ton)	V_{u80} (ton)
LP 02	23.0	59.2	117.0	4.5	2.299	3.448	2.758
LP 03	30.5	50.6	73.0	3.4	1.556	2.333	1.867
LP 04	16.6	41.3	66.1	3.7	1.935	2.903	2.322
LP 05	22.8	58.5	85.5	4.4	2.747	4.120	3.296
LP 06	12.8	25.4	43.9	4.0	1.724	2.586	2.069

The cracking pattern at the end of the tests is shown in figure 10. They are three-dimensional views of the specimens seen from the bottom. In the figures, the cracks are drawn with three colors, black represents cracks during the application of the axial load, blue, the pull cycle, and red, the push cycle. It can be seen that in the column there is no appreciable damage.

A summary of the most important tested parameters is shown in table 3. The type of failure that predominated in the tests was the punching shear. The interstory drift ratio associated with the failure is found in the order of 2%.

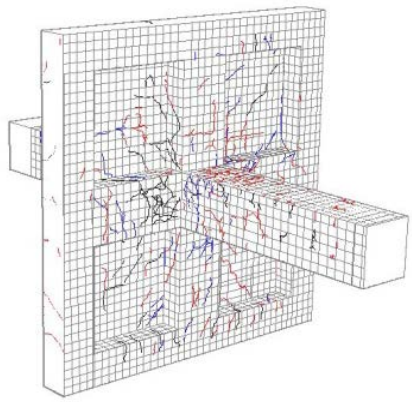

Fig. 11 – Cracking pattern at end of test LP-02

Table 3 – Interstory drift ratio at failure vs. Vu/VcR [2, 9]

Specimen	Reinforcement	V_u/V_{cR} (ACI-2011)	V_u/V_{cR} (NTC-2004)	Ψ	Failure
LP02	Stirrups	0.50	0.78	0.0202	Punching
LP03	SSR	0.52	0.86	0.0260	Punching
LP04	SSR	0.64	1.00	0.0230	Punching
LP05	SSR	0.49	0.82	0.0297	Flection
LP06	SSR	0.76	1.30	0.0182	Punching

The experimental results are shown in a graphic of the maximum interstory drift ratio vs normalized applied loads [10], see figure 11. The results of the five specimens are shown in the graphic, together with other results found in the literature. Each of the results of this study is shown twice, because the concrete resistance VcR was calculated with two methods: the NTC-Concreto, 2004, which does not take into account the effect of posttension stresses, and the ACI318-2011, where this effect is explicitly taken into account and increases the shear stresses resisted by the concrete.

The results of the waffle slabs tested in this research are below the results of the solid flat slabs tested by other authors [10] because there is less concrete around the column.

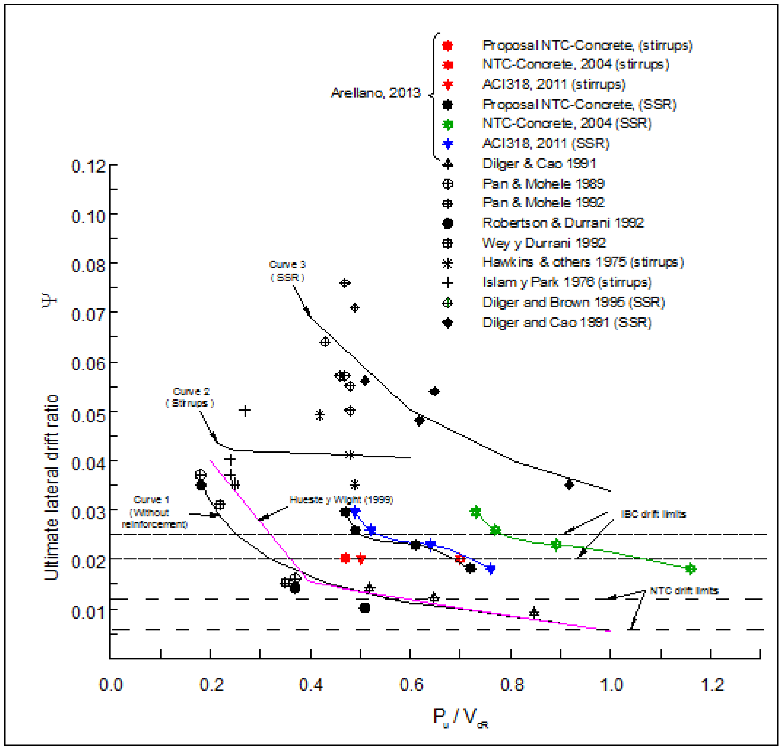

Fig. 12 – Effects of gravity loads on lateral drift capacity of interior slab-column connections (Joint ACI-ASCE, 2010)

5. Conclusions

Low values of the applied shear force may considerably improve the connection behavior. If the relation of Vu/VcR calculated with the NTC-Concreto [2], is limited to values less than 1.0, the connection may develop ultimate interstory drift ratio in the order of 2%, as is shown in the behavior of the elements LP-02, LP-03, LP-04, LP.05 and LP-06.

The tested specimens developed ductility ratios between 3.4 and 4.5 with the definition of the ductility in Section 3.6. The posttensioned waffle slab and columns system is very flexible and may develop interstory drift ratio similar to earthquake-resistant ductile systems.

When the relation of Vu/VcR is increased, the connection stiffness degrades more quickly. The specimen LP-05 is a special case because a flexural, rather than a punching shear, failure was developed. This means that larger deformations occur with stable cycles that dissipate more energy than that dissipated in punching shear failures.

In section 9.7.3 of the NTC-Concreto [2], which refers to posttensioned waffle slab-column structures under earthquakes, the allowable interstory drift ratio is limited to a value of 0.006. Taking into consideration the testing evidence of this research, this limit seems conservative and a larger one may be used for design.

Posttensioned waffle-slab and columns systems should not be used to dissipate energy, since the obtained tested hysteresis cycles were thin and present the pinching phenomenon around the origin, because the dominant failure mechanism was punching shear.

Both types of shear reinforcement used were suitable to resist the applied load at low levels of interstory drift ratio. When levels of interstory drift ratio larger to those allowed in ductile structures regulations were applied, problems arose in the connections with stud shear reinforcement (SSR), because SSR does not properly confine the longitudinal reinforcement bars in the ribs. Buckling of the bars occurred when the cover concrete was lost. Since current design regulations require designing for low interstory drift ratio (ψ=0.006), it may be said that with both types of reinforcement it is possible to reach similar deformations with the same safety. Shear stud reinforcement has an advantage in the co-location rate, but with the inconvenience that they may not confine properly the compression steel.

The use of posttensioned waffle slabs without a solid zone around the column is not recommended. Although this testing evidence seems to show that the system can reach deformation levels larger than those specified in the “Normas tecnicas complementarias para el diseño y construcción de estructuras de concreto NTC-Conceto [2], more studies are required before such recommendation can be made.

6. Acknowledgements

The sponsorship of Federal District Government in the development of this project is gratefully acknowledged, as the scholarship to pursue doctoral studies granted to Eduardo Arellano by CONACYT.

5. References

[1] NTC-Concreto, “Normas técnicas complementarias para el diseño y construcción de estructuras de concreto”, (1996), Gaceta Oficial del Distrito Federal, Sexta época, Tomo I, No. 356, México, 25 de Marzo de 1996. (In Spanish).

[2] NTC-Concreto, “Normas técnicas complementarias para el diseño y construcción de estructuras de concreto”, (2004), Gaceta Oficial del Distrito Federal, Décima cuarta época, Tomo I, No. 103-Bis, México, 6 de Octubre de 2004. (In Spanish, http://www.smie.org.mx/paginas/reglamentos/df/es_07.pdf)

[3] Megally, S. and Ghali, A. “Seismic behavior of slab-column connections” Canadian Journal of Structural Engineering, vol 27, pp 84-100, 2000.

[4] NTC-Sismo,”Normas técnicas complementarias para el diseño por sismo”, (2004), Gaceta Oficial del Distrito Federal, Décima cuarta época, Tomo II, No. 103-Bis, México, 6 de Octubre de 2004. (In Spanish, http://www.smie.org.mx/paginas/reglamentos/df/es_08.pdf)

[5] Chopra A. K. (2000), “Dynamics of structures” Prentice Hall, USA, pp. 98-105.

[6] Ghali, A. “Seismic-resistant joints of interior columns with prestressed slabs”, ACI Structural Journal, Vol. 103, No. 5, pp 710-719, 2006.

[7] Pan, A., and Moehle, L.P., “Lateral Displacement Ductility of Reinforced Concrete Flat-Slabs”, ACI Structural Journal, Vol. 86, No. 3, pp 250-258, 1989.

[8] Kuramoto, H. and Nishiyama I., “Equivalent Damping Factor of Composite RCS Frames” ACI , SP196-06 pp 109-124, 2000.

[9] ACI Committee 318, “Building code requirements for structural concrete”, ACI, Farmington Hills, Mi. USA, 2015.

[10] Joint ACI-ASCE Committee 421, “Seismic design of punching shear reinforcement in flat plates ACI 421.2R-10)”, ACI, Farmington Hill, Mich., pp. 1-26, 2010.